HHS Public Access

Author manuscript

Nature. Author manuscript; available in PMC 2012 October 26.

Published in final edited form as:

Nature. ; 484(7395): 510–513. doi:10.1038/nature11012.

NLRP10 is a NOD-like receptor essential to initiate adaptive immunity by dendritic cells

Stephanie C. Eisenbarth[1,*,☜], **Adam Williams**[2,☜], **Oscar R. Colegio**[3], **Hailong Meng**[4], **Till Strowig**[2], **Anthony Rongvaux**[2], **Jorge Henao-Mejia**[2], **Christoph A. Thaiss**[2], **Sophie Joly**[6], **David Gonzalez**[1], **Lan Xu**[1,3], **Lauren A. Zenewicz**[2], **Ann M. Haberman**[1], **Eran Elinav**[2], **Steven H. Kleinstein**[4,5], **Fayyaz S. Sutterwala**[7,8], and **Richard A. Flavell**[2,6,*]

[1]Department of Laboratory Medicine, Yale University School of Medicine, New Haven, CT 06520, USA

[2]Department of Immunobiology, Yale University School of Medicine, New Haven, CT 06520, USA

[3]Department of Dermatology, Yale University School of Medicine, New Haven, CT 06520, USA

[4]Department of Pathology, Yale University School of Medicine, New Haven, CT 06520, USA

[5]Interdepartmental Program in Computational Biology and Bioinformatics, Yale University School of Medicine, New Haven, CT 06520, USA

[6]Howard Hughes Medical Institute, Yale University School of Medicine, New Haven, CT 06520, USA

[7]Inflammation Program, Department of Internal Medicine, University of Iowa, Iowa City, IA 52242, USA

[8]Veterans Affairs Medical Center, Iowa City, IA 52241, USA

Abstract

NLRs (nucleotide-binding domain leucine-rich repeat containing receptors; NOD-like receptors) are a class of pattern recognition receptor (PRR) that respond to host perturbation from either infectious agents or cellular stress[1,2]. The function of most NLR family members has not been

[*]Correspondence to: Stephanie C. Eisenbarth, Department of Laboratory Medicine, Yale School of Medicine, 300 George St. 353D, New Haven, CT 06511; Phone: (203) 737-4188; Fax: (203) 737-2704; stephanie.eisenbarth@yale.edu. [*]Correspondence to: Richard A. Flavell, Department of Immunobiology, Yale University School of Medicine, TAC S-579, New Haven, CT 06520; Phone: (203) 737-2216; Fax: (203) 737-2958; richard.flavell@yale.edu.

[☜]These authors contributed equally to this work.

The authors report no conflict of interest.

Author contribution

S.C.E. and A.W. wrote the manuscript, designed, performed and interpreted experiments with technical assistance from L.X., F.S.S. generated *Nlrp10*$^{-/-}$ mice, S.J. performed *in vitro* inflammasome activation, O.R.C. and J.H-M. assisted with transwell assays and performed real time PCR, L.A.Z. assisted with EAE experiments, T.S. assisted with TNP immunizations, A.R. assisted with i.v. LPS experiments, E.E. provided technical assistance with DC isolations, C.A.T. performed immunofluorescence experiments, H.M. and S.H.K. performed array analysis, D.G. and A.M.H. performed intravital microscopy and quantification. R.A.F. assisted in experimental design and interpretation.

The microarray data discussed in this publication have been deposited in NCBI's Gene Expression Omnibus and are accessible through GEO Series accession number GSE36009.

characterized and their role in instructing adaptive immune responses remains unclear [2,3]. NLRP10 (also known as PYNOD, NALP10, PAN5 and NOD8) is the only NLR lacking the putative ligand binding leucine rich repeat domain, and has been postulated to be a negative regulator of other NLR members including NLRP3[4–6]. We did not find evidence that NLRP10 functions through an inflammasome to regulate caspase-1 activity nor that it regulates other inflammasomes. Instead, *Nlrp10*$^{-/-}$ mice had a profound defect in helper T cell-driven immune responses to a diverse array of adjuvants including lipopolysaccharide (LPS), aluminium hydroxide (alum) and complete Freund's adjuvant (CFA). Adaptive immunity was impaired in the absence of NLRP10 due to a dendritic cell (DC) intrinsic defect in emigration from inflamed tissues while upregulation of DC costimulatory molecules and chemotaxis to CCR7-dependent and independent ligands remained intact. The loss of antigen transport to the draining LN by this migratory DC subset resulted in an almost absolute loss in naïve CD4^{+} T cell priming, highlighting the critical link between diverse innate immune stimulation, NLRP10 activity and the immune function of mature DCs.

Keywords

Adjuvants; Alum; EAE; Multiple Sclerosis; Asthma; Complete Freund's Adjuvant; NOD-like Receptors; Nalp; Caspase-1; Pattern Recognition Receptor

---

To elucidate the *in vivo* biologic role of NLRP10, we generated mice deficient in NLRP10 (Supplementary Fig. 1a–c). *Nlrp10*$^{-/-}$ mice appeared healthy without evidence of autoimmunity or tumour formation and had a normal composition and activation profile of immune cells including T and B lymphocytes in the periphery, bone marrow and thymus (data not shown). Peritoneal macrophages or bone marrow derived dendritic cells (BMDC) from *Nlrp10*$^{-/-}$ mice stimulated with Toll-like receptor (TLR) agonists or NLRP3 inflammasome activators secreted normal levels of IL-1β, TNF-α and IL-6 (Supplementary Fig. 2a–c) indicating that loss of NLRP10 does not affect caspase-1 or NLRP3 inflammasome function. To test *in vivo* whether NLRP10 acts as a negative regulator of NLRs, we tested the ability of *Nlrp10*$^{-/-}$ mice to mount antigen-specific immune responses to OVA and alum in a Th2-driven asthma model [7,8] or CFA (mycobacteria-based) with MOG peptide in the Th17-driven model of experimental autoimmune encephalomyelitis (EAE) [9]. Surprisingly, *Nlrp10*$^{-/-}$ mice had a profound defect in adaptive immunity in both models. Th2 responses in the lung, LN and systemic antibody production were significantly reduced in *Nlrp10*$^{-/-}$ mice (Fig. 1a–c & Supplementary Fig. 3a). Similarly, most *Nlrp10*$^{-/-}$ mice completely failed to develop signs of EAE and exhibited a marked reduction in MOG-specific IL-17 and IFN-γ production from the spleen, LNs and spinal cord (Fig. 1d–f & Supplementary Fig. 3b). Most surprisingly, immunization using only LPS as an adjuvant in an intranasal Th1/neutrophil airway inflammation model [10] was also defective in *Nlrp10*$^{-/-}$ mice (Fig. 1g). Altogether these findings suggest that *Nlrp10*$^{-/-}$ mice have a global defect in adaptive immunity upon immunization with multiple adjuvants. Bone marrow chimeric mice in which NLRP10 deficiency was limited to the hematopoietic compartment failed to respond to OVA/alum immunization, demonstrating that loss of NLRP10 in bone marrow derived cells was sufficient to recapitulate the phenotype (Fig. 2a–c).

To test if the *Nlrp10*$^{-/-}$ mice have a defect in T cell driven adaptive immune processes, we compared the immunization response to the hapten trinitrophenyl (TNP) linked to either KLH or Ficoll. In this model, anti-TNP antibodies are generated by activated B cells in either a T cell-dependent (KLH) or T cell-independent (Ficoll) manner [11,12]. Anti-TNP IgG1 antibodies were severely diminished with TNP-KLH (Fig. 2d) but there was no defect in T cell-independent IgG3 (Fig. 2e) antibody production to TNP-Ficoll. Therefore, *Nlrp10*$^{-/-}$ B cells are not intrinsically impaired but T cell activation, either secondary to a T cell intrinsic or T cell extrinsic defect, is severely impaired in *Nlrp10*$^{-/-}$mice. *Nlrp10*$^{-/-}$ T cells can be primed and differentiated into cytokine producing helper T cell subsets (Supplementary Fig. 4) *in vitro*. Further, adoptively transferred TCR transgenic, *Nlrp10*$^{-/-}$ OTII T cells proliferated normally in wild-type (WT) hosts following cognate antigen immunization (OVA) (Supplementary Fig. 5). Therefore, we concluded that *Nlrp10*$^{-/-}$ mice fail to initiate adaptive immune responses possibly due to a T cell extrinsic defect in antigen presentation.

To evaluate T cell priming *in vivo*, we adoptively transferred CFSE-labelled naïve WT TCR transgenic OTII T cells into WT and *Nlrp10*$^{-/-}$ mice. Following immunization with cognate protein antigen, these WT T cells divided only in WT but not *Nlrp10*$^{-/-}$ hosts (Fig. 2f), suggesting that the injected antigen was not being presented to naïve T cells in the absence of NLRP10. As dendritic cells are the primary antigen presenting cell (APC) controlling the activation fate of naïve T cells following immunization, we tested whether DC maturation was defective in *Nlrp10*$^{-/-}$ mice [13]. *Nlrp10*$^{-/-}$ BMDCs *in vitro* and splenic DCs *in vivo* upregulated all requisite stimulatory molecules necessary for effective T cell priming, including MHC class II and B7 family members (CD86) following LPS exposure (Supplementary Fig. 6a, 6d and data not shown). Similarly *Nlrp10*$^{-/-}$ DCs efficiently phagocytosed fluorescently labelled OVA *in vitro* (Supplementary Fig. 6b) and *in vivo* (Supplementary Fig. 6e). Antigen-pulsed *Nlrp10*$^{-/-}$ BMDCs were also capable of activating naive CFSE-labelled WT OTII T cells *in vitro* (Supplementary Fig. 6c). Therefore DC maturation following innate stimulation was intact; yet *Nlrp10*$^{-/-}$ BMDCs loaded with protein antigen and adoptively transferred into mice harbouring CFSE-labelled naïve OTII T cells were unable to activate these T cells (Fig. 3a) suggesting that the T cell priming defect in *Nlrp10*$^{-/-}$ mice was due to a loss of DC-T cell interactions. To test this, we used the traditional model of FITC skin painting to track migration of DCs from the skin to the LN [14]. FITC painted *Nlrp10*$^{-/-}$ mice contained few FITC^{+} DCs in the draining LN at 18 hours, similar to mice lacking the critical LN homing chemokine receptor CCR7 [14–16] (Fig. 3b and Supplementary Fig. 7). However, FITC^{+} DCs were present in the ear in both WT and *Nlrp10*$^{-/-}$ mice (data not shown), suggesting that *Nlrp10*$^{-/-}$ DCs were viable and capable of capturing antigen but failed to reach the LN. *Nlrp10*$^{-/-}$ mice also demonstrated a profound absence of antigen-containing DCs in the draining LN following subcutaneous injection of a fluorescently labelled antigen (0.5 – 5.0 ug OVA-AF647) at 18 hours (Fig. 3c) or any timepoint evaluated out to 12 days following immunization (data not shown). This defect in antigen-containing DCs in the LN could be partially overcome in *Nlrp10*$^{-/-}$ mice upon exposure to high antigen doses (e.g., 50 μg OVA) (Fig. 3c), as previously observed in CCR7-deficient mice [14]. This is likely a result of passively drained antigen to the LN, which initiates weak T cell responses [14,17]. Evaluation of mediastinal LNs after inhalation of particulate latex beads that cannot passively drain to LNs clearly indicated that *Nlrp10*$^{-/-}$

DCs were unable to traffic antigen to the draining LN, yet bead-containing DCs were present in the lung (Supplementary Fig. 8). Therefore *Nlrp10*$^{-/-}$ mice have a profound defect in DC-dependent trafficking of antigen to lymph nodes. Lymphoid tissue resident CD8α^{+} and plasmacytoid DCs were not different between WT and *Nlrp10*$^{-/-}$ mice (Supplementary Fig. 7 and data not shown) as would be expected, given that they enter the LN via the blood stream. In contrast, migratory DCs which take antigen from inflamed tissue to the LN[18] and express high levels of MHC class II but intermediate CD11c, were affected by the loss of NLRP10. Specifically, within this group we found that the CDllb^{+}CD207^{-}CD103^{-} DC subset, which is primarily responsible for priming helper T cells, is nearly absent in the LN of immunized *Nlrp10*$^{-/-}$ mice (Supplementary Fig. 7) again similar to the defect observed in CCR7-deficient mice[14,19–21]. Consistent with the finding that antigen-containing mature DCs were present normally in the ear or lung of immunized *Nlrp10*$^{-/-}$mice (Supplementary Fig. 8), we found no DC subset deficiency in any non-lymphoid tissue from knockout mice (Supplementary Fig. 9) indicating that the development and migration of CD11b^{+} DCs to peripheral tissues is intact in the absence of NLRP10. To determine whether the defect in DC migration to the LN is cell intrinsic or extrinsic, we co-injected labelled activated WT and *Nlrp10*$^{-/-}$ BMDCs into WT or *Nlrp10*$^{-/-}$ host mice. Although WT DCs were found in the LN 18 hours after subcutaneous injection, very few *Nlrp10*$^{-/-}$ DCs were present (Fig. 3d), regardless of the presence or absence of NLRP10 in the host (Supplementary Fig. 10), confirming that *Nlrp10*$^{-/-}$ DCs were incapable of reaching the LNs due to a cell intrinsic defect. Altogether, we conclude that NLRP10 is essential for DC-mediated trafficking of antigen to the LN from multiple peripheral sites following maturation by a wide range of innate stimuli.

Given the similarity of our findings to those described for CCR7-deficient mice, we postulated that *Nlrp10*$^{-/-}$ DCs might have a defect in CCR7 expression. However, *Ccr7* mRNA (Supplementary Fig. 11a) and CCR7 surface expression (Fig. 4a) in LPS-treated *Nlrp10*$^{-/-}$ BMDCs was equivalent to WT BMDCs. Consistent with CCR7 expression, *Nlrp10*$^{-/-}$ DCs responded normally *in vitro* to a gradient of CCL19 and CCL21 as well as a CCR7 independent chemokine CXCL12 (SDF-1) and the signalling sphingolipid S1P[14,22,23] in transwell assays (Fig. 4b & Supplementary Fig. 11b–c), indicating CCR7 sensing and signalling was intact and that general DC kinesis was not affected in *Nlrp10*$^{-/-}$ mice. Despite the apparently normal homing properties of *Nlrp10*$^{-/-}$ DCs *in vitro*, splenic DCs failed to relocalize to the T cell zone in the spleen following LPS stimulation *in vivo* (Supplementary Fig. 12). DC relocalization requires numerous integrated steps including emigration from the initial site of residence, the ability to home towards a chemokine gradient, transmigration through the lymphatic endothelial layer and the physical machinery to do so [15,24–26]. Yet we found no defect in the ability of *Nlrp10*$^{-/-}$DCs to traverse an endothelial monolayer, to polymerize actin or general kinesis on a fibroblast cell layer (data not shown). As homing towards CCR7 ligands and S1P was intact *in vitro*, we postulated that NLRP10 regulates the emigration of DCs from inflamed tissue. To visualize DC movement *in vivo* we used 2-photon laser scanning microscopy to follow co-injected fluorescently labelled WT and *Nlrp10*$^{-/-}$ DCs in WT hosts (Supplementary Movie 1–2). Tracking the movement of individual DCs within the tissue using Imaris software revealed that WT DCs actively moved away from the injection site and surveyed the surrounding

tissue whereas the majority of *Nlrp10*$^{-/-}$ DCs remained near the site of injection despite their active extension of lamellipodia (Fig. 4c).

Altogether these experiments indicate that the loss of NLRP10 in DCs impairs their ability to exit inflamed tissues, suggesting a defect in a molecular pathway regulating the detachment of dendritic cells from extracellular matrix components. Yet we did not observe altered surface expression of particular adhesion molecules including β1, β2 or β3 integrin chains, DC-SIGN nor altered *in vitro* adhesion to ICAM-1, ICAM-2, fibronectin or Collagen I (data not shown). However, such surface expression or isolated *in vitro* adhesion assays will not reveal defects in chemokine receptor-integrin activation pathways. Therefore to identify novel molecules potentially involved in NLRP10-dependent DC function we used an unbiased gene array approach on *Nlrp10*$^{-/-}$ BMDCs treated with or without LPS. We discovered that only 24 genes were differentially expressed (q value < 0.05 and absolute fold-change > 1.2) in *Nlrp10*$^{-/-}$ DCs as compared to WT DCs (Fig. 4d). Restricting the analysis to genes that were more than two fold up/down regulated at baseline and after LPS stimulation revealed only three differentially expressed genes: *Il4ra*, *Mmp13* and *Gdpd3* (Supplementary Fig. 13). The first two genes identified were either not differentially expressed on *Nlrp10*$^{-/-}$ DCs at the protein level or do not regulate DC-dependent immunization[27] (Supplementary Fig. 13a–b). We were most intrigued by the aberrant regulation of a molecule with no known mammalian function, glycerophosphodiester phosphodiesterase domain containing 3 (GDPD3) (Supplementary Fig. 13c), because its domain structure suggests it has multiple transmembrane regions and structural homology to glycerophosphodiester phosphodiesterase 1 (GDE1). *Gdpd3* was more than 80-fold upregulated in *Nlrp10*$^{-/-}$BMDCs as compared to WT DCs by RT-PCR (Supplementary Fig. 13c). GDPD family members catalyse the hydrolysis of glycerophosphoinositol, but in addition have functions in cell morphology, motility and G protein signalling downstream of chemokine receptors [28] indicating a potential link between NLR activity, phospholipid metabolism and the motility of mature DCs. Subsequent work characterizing GDPD3 will potentially provide important clues on how NLRP10 regulates a fundamental cellular process in DCs during inflammation. Although no other NLR or TLR reported to date affects adaptive immunity globally in this way, there is a growing body of literature to indicate multiple NLRs and related signalling molecules are involved in controlling different aspects of DC function[29,30]. The finding that inhibition of a single NLR, NLRP10, can paralyze mature DCs could have a profound impact on the approach to treating misguided adaptive immune responses driving allergy and autoimmunity.

Methods Summary

For asthma models, mice were sensitized by either intraperitoneal injection of OVA/alum or intranasal OVA. Mice were then challenged intranasally with OVA. EAE was elicited using MOG peptide, CFA, heat-inactivated *Mycobacterium tuberculosis* and *Bordetella pertussis* toxin. For TNP immunizations, TNP-KLH or TNP-Ficoll was administered i.p. and serum analysed for anti-TNP antibodies by ELISA. For intravenous LPS delivery, mice given LPS by retro-orbital injection were bled at 90 minutes and 6 hours and serum analysed by ELISA. Spleens were analysed by flow cytometry at 6 hours. For antigen tracing, Alexa Fluor 647-OVA and LPS were co-injected subcutaneously and 18 hours later lymph nodes

were analysed by flow cytometry. For DC transfer labelled BMDCs were co-injected into the flank of WT mice, and draining lymph nodes were analysed by flow cytometry. For *in vivo* OTII T cell stimulation, OVA peptide loaded BMDCs were injected subcutaneously, and inguinal LNs harvested three days later to evaluate T cell proliferation. For intravital microscopy, labelled BMDCs were co-injected intradermally and imaged using an upright two-photon laser scanning microscope, and quantified using Imaris software. For gene expression analysis an Affymetrix Mouse Gene 1.0 ST Array was used.

Methods

Materials

All reagents were purchased from Sigma except Imject alum (Pierce) and IFA (Difco) unless indicated otherwise. Antibody pairs for ELISA were purchased from R&D Systems (IL-1β), BD Pharmingen (IL-5, IL-6, IL-17 and IFN-γ) or from eBioscience (TNF-α. OVA-specific IgG1 was measured by ELISA as previously described [10] and secondary antibodies were purchased from BD Pharmingen. TNP-specific IgG3 and IgG1 was performed as above with TNP-OVA used for coating instead of OVA and HRP-conjugated secondary antibodies (Bethyl).

Mice

To generate mice specifically deficient in *Nlrp10* exons 2 and 3 of the *Nlrp10* gene, containing the translation-initiation codon ATG, were replaced by a *neo* cassette flanked by two *loxP* sites (Supplementary Figure 1a). The *Nlrp10* targeting vector was electroporated into C57BL/6 embryonic stem (ES) cells (Bruce4). Homologous recombinant ES cells were identified by Southern blot analysis and were microinjected into BALB/c blastocysts. Chimeric offspring were backcrossed to C57BL/6 mice, and germline transmission was confirmed by PCR of tail genomic DNA. Screening of $Nlrp10^{-/-}$ mice with the primers 5′-TAGAGTGGATACCCAGCACACACG-3′ and 5′-CATCTCGTAAGTGGAACTTCAGCG-3′ amplifies a 700 bp product from the WT allele; primers 5′-TAGAGTGGATACCCAGCACACACG-3′ and 5′-AACGAGATCAGCAGCCTCTGTTC-3′ amplify a 594 bp product from the targeted allele. RT-PCR analysis of cDNA isolated from $Nlrp10^{+/+}$ and $Nlrp10^{-/-}$ splenocytes confirmed the absence of *Nlrp10* mRNA in $Nlrp10^{-/-}$ mice. Primers used for RT-PCR analysis were as follows: *Nlrp10*, 5′-GGAGCTTGTAGACTACCTCA-3′, 5′-AAAGTCTCCACATCGACAGG-3′; *Hprt*, 5′-GTTGGATACAGGCCAGACTTTGTTG-3′, 5′-GAGGGTAGGCTGGCCTATAGGCT -3′.

The generation of mice deficient in NLRP3 have been reported previously [31]. Age and sex-matched C57BL/6 (CD45.2) mice from the National Cancer Institute were used as all WT controls. All naïve mice were C57BL/6 unless otherwise indicated in the figure. RAG1-deficient (B6.129S7-$Rag1^{tm1Mom}$/J) and OTII (B6.Cg-Tg(TcraTcrb)425Cbn/J) and CCR7-deficient mice were purchased from Jackson Labs. OTII mice were crossed onto the $Rag1^{-/-}$ and CD45.1 (B6Ly5.2Cr) background from NCI. All protocols used in this study were approved by the Yale Institutional Animal Care and Use Committee.

Asthma Model

For intraperitoneal sensitization, 6–8-week-old mice were injected intraperitoneally on day 0 with 50 μg of ovalbumin (Grade V; Sigma) adsorbed on 2 mg of Imject alum and again on day 10 with 25 μg of ovalbumin adsorbed on 2 mg of Imject alum. Mice were challenged intranasally with 25 μg of ovalbumin in PBS on days 21, 22 and 23 and sacrificed for analysis on day 25. For sensitization by inhalation, 100 μg Ova with an additional 0.05 μg LPS in 50 μL PBS was given intranasally on days 0, 1 and 2 as previously described [10]. Mice were challenged intranasally with 25 μg of Ova in PBS on days 14, 15, 18 and 19 and sacrificed on day 21 for analysis. Naïve mice (WT) were not sensitized i.p. but received an i.n. OVA challenge.

Bronchoalveolar lavage analysis

Mice were primed and challenged as indicated. On the day of analysis, mice were sacrificed and bronchoalveolar lavage was performed as described previously [32]. In brief, inflammatory cells in the airways were obtained by cannulation of the trachea and lavage of the airway lumen with 3 mL PBS. Red blood cells were lysed and total cell numbers were counted with a haemocytometer and cytospin slides were prepared by haematoxylin and eosin staining with Diff-Quick (Dade Behring Inc.).

Ex vivo lymphocyte restimulation

Draining lymph nodes (inguinal or mediastinal) were removed and single cells suspensions were generated. 5×10^6/mL lymph node cells were cultured with 5×10^6/mL antigen presenting cells (see below) in the presence or absence of 200μg/ml of OVA for 48 hours. Syngeneic T cell depleted splenocytes were used as antigen-presenting cells and were prepared by complement lysis using antibodies to CD4 (GK1.5), CD8 (TIB105) and Thy1 (Y19), followed by treatment with mitomycin C.

Experimental Autoimmune Encephalomyelitis Model

EAE was elicited and scored as previously described [33]. Briefly, on day 0 mice received bilateral subcutaneous flank injection of 50 μg of MOG (MEVGWYRSPFSRVVHLYRNGK) peptide in complete Freund's adjuvant (CFA) containing 500 μg of heat-inactivated *Mycobacterium tuberculosis* (Difco Labs). A dose of 200 ng of *Bordetella pertussis* toxin (PT; LIST Biological Labs) was injected i.p. on days 0 and 2. Mice were monitored daily and scored as follows: 1, flaccid tail; 2, partial unilateral hindlimb paralysis or inability to right; 3, complete unilateral hindlimb paralysis; 4, complete bilateral hindlimb paralysis; and 5, moribund. After disease resolution (a majority of the paralysis resolved), mice were challenged with 50 μg MOG peptide i.p. with 200 ng PT in PBS. 4 days later, spleen and inguinal LNs were harvested, pooled and 5×10^6 cells were stimulated with 10 μg/mL MOG peptide and an equal number of syngeneic T cell depleted splenocytes (as described below). 48 hours later, supernatant was collected for cytokine analysis by ELISA. Naïve mice (WT) did not receive MOG peptide.

TNP Model

300 μg TNP-KLH (29:1) and 100 μg TNP-Ficoll (90:1) (both from Biosearch Technologies) were administered i.p. in PBS on day 0 and 14. Mice were sacrificed on day 30 and anti-TNP antibodies were analysed by ELISA from serum.

Intravenous LPS Model

Mice were given 25 μg of LPS by retro-orbital injection. Mice were bled at 90 minutes and 6 hours and spleens were removed at 6 hours. Spleens were treated with collagenase D (Roche) at 37 °C for 45 minutes, red blood cells were lysed and samples were stained and analysed by flow cytometry. Blood was allowed to clot at room temp, serum isolated and analysed by ELISA.

Subcutaneous OVA-AF647

Indicated amounts of Alexa Fluor 647-OVA (OVA-AF647, Molecular Probes) were injected with 10 μg LPS subcutaneously in the flank bilaterally of WT and *Nlrp10*$^{-/-}$ mice. 18 hours post injection inguinal lymph nodes were removed, digested with collagenase D for 1 hour at 37 °C and stained for flow cytometry analysis.

DC Transfer Experiments

BMDCs were labelled with either 2 μM CFSE or 2 μM CellTrace Violet at 37 °C for 5 minutes. 3 × 10^6 labelled BMDCs were mixed in equal numbers and 3×10^6 BMDC were injected into each flank of CD45.1 C57BL/6 mice. After 1 day, draining inguinal lymph nodes were removed, digested with collagenase D for 1 hour and 37 °C before antibody staining and analysis by flow cytometry. For *in vivo* OTII T cell stimulation, WT or *Nlrp10*$^{-/-}$ BMDCs were loaded for 1 hour with OVA peptide (ISQAVHAAHAEINEAGR) or nothing, extensively washed and 1×10^6 were injected subcutaneously in the flank. Inguinal LNs were harvested three days later to evaluate T cell proliferation.

Bone marrow chimeras

Bone marrow was flushed from femurs, red cells were lysed and filtered through a 70-μm filter. 1×10^6 cells in 100 μL PBS were delivered by retro-orbital injection into lethally irradiated (1000 rad) mice. For two weeks post engraftment mice were maintained on antibiotics and six weeks after transplant, chimerism was assessed using congenic CD45 markers. All mice used in the experiments demonstrated at least 92% hematopoietic engraftment.

T cell proliferation studies

From the spleen and LNs of OTII transgenic mice on a RAG1-deficient background, $CD4^+$ cells were prepared by positive selection using CD4 Miltenyi beads (L3T4) per the manufacturer's instructions. CD4 positive cells were labelled with CFSE (2 μm; Molecular Probes) for 5 minutes at 37°C and then washed once in FBS and twice with PBS. For *in vivo* studies 3×10^6 cells were transferred into mice by retro-orbital injection. After one day, mice were challenged by subcutaneous injection of 0.25 μg OVA protein with either 100 μL CFA or 5 μg LPS in each flank and 3 days later, inguinal LNs were removed and analysed by

flow cytometry. For *in vitro* studies 1×10^5 OTII T cells were stimulated with 1×10^4 WT or *Nlrp10*$^{-/-}$ BMDCs loaded with 100 μg OVA or BSA in a 96 well plate for 3 days.

In vitro T cell activation and skewing

For *in vitro* T cell skewing, polyclonal WT or *Nlrp10*$^{-/-}$ T cells were stimulated with plate bound anti-CD3 (10 μg/mL) and anti-CD28 (2μg/mL). T cell skewing was accomplished for Th1 cultures with IL-12 (3.5 ng/mL), IL-2 (0.1 ng/mL) and anti-IL-4 (10 μg/mL); for Th2 cultures with IL-4 (20 ng/ml), IL-2 (0.1 ng/mL) and anti-IFN-γ (10 μg/mL); for Th17 cultures with IL-6 (20 ng/mL), IL-23 (20 ng/mL), TGFβ (0.5 ng/mL) and anti-IFN-γ (10 μg/mL; XMG1.2) and anti-IL-4 (10 μg/mL;11B11). After 5 days, cells were collected and restimulated with plate bound anti-CD3 (10 μg/mL) for 8 hours and supernatant was analysed by ELISA.

Flow cytometry protocols and antibodies

CD11b (M1/70), CD45.1 (A20), Valpha2 TCR (B20.1), CD4 (RM4-5), CD19 (6D5), CD3e (145-2C11), CD86 (GL1) flow cytometry antibodies were from BD. CDllc (N418), CD45.2 (104), B220 (RA3-6B2) were from Biolegend. I^AI^E (M5/114.15.2) was from eBioscience. Intracellular cytokine staining was done using the BD Cytofix/Cytoperm kit and according to manufacturers protocol. IL-17A (TC11-18H10) and IFN-γ (XMG1.2) were both from BD. 5-(and-6) carboxyfluorescein diacetate, succinimidyl ester (CFSE) from Invitrogen. CCR7 staining was performed on BMDCs after FcR blocking using a PE-conjugated anti-CD197 (clone 4B12) antibody from BD Pharmingen at 1:100 at 37 °C for 40 minutes.

In vitro DC and macrophage stimulation

The generation of thioglycollate-elicited peritoneal and bone-marrow-derived macrophages and bone-marrow-derived dendritic cells has been described previously[31,34]. For Supplementary Figure 2a, cells were primed by stimulating with 50 ng/mL LPS from *Escherichia coli* serotype 0111:B4 (Invivogen) for 16–18 hours before stimulation ATP or alum. For ATP-stimulated cells, the medium was changed at 20 min. and all stimulants were replaced. All other TLR ligands were used at the concentration indicated in the figure legend. Type A CpG (Invivogen), heat-killed *M. tuberculosis* (Difco), PolyI:C (Amersham) and Imiquimod (R837; Invivogen). To assess antigen processing, BMDCs were incubated with 2 μg/mL Alexa Fluor 647-OVA for 1 hour at 37 or 4 °C. Cells were then washed, stained with antibodies and analysed by flow cytometry.

Relative gene expression analysis

RNA from cells was isolated using Trizol (Invitrogen) and RNA was subjected to reverse transcriptase with Superscript II (Invitrogen) with oligo(dT) primer in accordance with the manufacturer's protocol. cDNA was quantified using commercially available primer/probe sets (Applied Biosystems) by real-time PCR and analysed with the ΔC_t (change in cycle threshold) method. All results were normalized to *Hprt* quantified in parallel amplification reactions during each PCR quantification. Results are presented as levels relative to *Hprt*. The following primer/probes were used: *Ccr7* Mm1301785_m1, *Gdpd3* Mm00470322_m1, *Il4ra* Mm00439634_m1, *Mmp13* Mm00439491_m1, *Hprt* Mm00446968_m1.

Intravenous antigen injection

5 μg of Alexa Fluor 647-OVA (molecular probes) was administered i.v. by retro orbital injection. After 4 hours spleens were harvested and treated with collagenase D and DNAse I at 37 °C for 45 minutes, red cells were lysed and samples were stained and analysed by flow cytometry.

Intranasal latex bead delivery

Yellow-green fluorescent 0.5 μm latex particles (Polysciences) were diluted 1/25 in PBS and 50ul was administered intranasally with 1 μg LPS[35]. 18 hours later draining mediastinal lymph nodes were harvested and digested with collagenase D before staining and analysis by flow cytometry. In parallel, lung was minced into small pieces, incubated with a cocktail of 150 U/mL Collagenase type I (Worthington Biochemical Corp) and 20 μg/mL DNAse I in media supplemented with 10% FBS for 30 minutes at 37 °C. After passing through a 70 μm mesh, the single cell suspension was stained and analysed by flow cytometry.

FITC painting

The ventral portion of each ear was painted with 20ul of 1% fluorescein isothiocyanate (FITC) in carrier solution (1:1 v/v acetone:dibutyl phthalate) [14,23]. After 18 hours draining lymph nodes were harvested, digested with collagenase D, stained and analysed by flow cytometry. In parallel, ears were split into dorsal and ventral halves and floated dermal side down on dispase (2 mg/mL, Roche) for 30 min at 37 °C. Ears were then minced and incubated in the presence of collagenase D (5 mg/mL), DNAse I (0.1 mg/ml) and hyaluronidase (2 mg/mL MP Biomedicals) for 30 min at 37 °C. After passing through a 70 μm mesh the resulting single cell suspension was stained and analysed by flow cytometry.

Transwell assay

BMDCs stimulated with LPS (1 μg/mL) overnight were harvested, washed twice in ice cold PBS before suspension in RPMI supplemented with 0.1% fatty acid free BSA (Sigma). Chemokines were suspended in RPMI supplemented with 0.1% fatty acid free BSA at 100 ng/mL. 600ul of each was added into a 24 well non-tissue culture treated plate containing a 6.5mm Transwell insert with a 5.0 μm pore size (Corning), and allowed to equilibrate for 30–45 minutes in tissue culture incubator before the addition of 100 μL of cells at a concentration of 1×10^7 mL to the upper chamber. After 3 hours migrated cells were harvested from the lower chamber and counted using a haemocytometer. For pertussis toxin treatment cells were cultured overnight in the presence of pertussis toxin (100 ng/mL). For controls BMDCs were in media containing respective chemokines before adding to the upper chamber.

Intravenous LPS and spleen immunofluorescence staining

WT and *Nlrp10*$^{-/-}$ mice were injected with 5 μg of LPS and after 4 hours spleens were removed and fixed with 4% PFA solution for 4 hours at 4°C and then treated with increasing concentrations of sucrose (up to 30% in PBS) over night. Organs were embedded in O.C.T. compound (Sakura), and 5 μm cryosections from frozen tissue blocks were prepared using a cryostat (Leica) at a working temperature of −19°C. Frozen sections of were blocked in 5%

fetal bovine serum for 30 minutes at room temperature. Slides were incubated at 4°C with primary antibodies to CD3 (clone17A2, BD Pharmingen) and CD11c (biotinylated, clone HL3, BD Pharmingen) followed by incubation with AlexaFluor 647-labeled chicken anti-rat IgG (Molecular Probes) and PE-labeled streptavidin Biolegend) for 2 hours at room temperature. Slides were then dried and mounted using ProLong Antifade mounting medium (Invitrogen,). Images were acquired on a PerkinElmer Ultraview Spinning disk confocal microscope and images were processed using Volocity software (PerkinElmer).

Intravital microscopy

BMDCs stimulated with LPS (1 μg/mL) overnight were harvested, washed twice in ice cold PBS before staining with either CFSE or CMTMR (Molecular Probes). After washing twice with fetal calf serum and twice with PBS, 0.5–1×10^5 cells in 10 μL of PBS and 2.5 μg LPS were injected intradermally into each ear (with or without an equal mixture of unlabelled DCs). Imaging of dendritic cell motility in ear skin of mice was performed using an upright two-photon laser scanning microscope. For image acquisition, an Olympus BX61WI fluorescence microscope with a 20X, 0.95NA water immersion Olympus objective and dedicated single beam LaVision TriM laser scanning microscope (LaVision Biotec) was controlled by Imspector software. The microscope was outfitted with a Chameleon Vision II Ti:Sapphire laser (Coherent) with pulse pre-compensation. Emission wavelengths of 390 – 480 nm (blue, for second harmonic generation emissions), 500 – 550 nm (green, CFSE), and 565 – 665 nm (orange-red, for CMTMR) were collected with an array of 3 photomultiplier tubes (Hamamatsu). Mice were anesthetized with an i.p. injection of ketamine (100 mg/kg) and xylazine (10mg/kg) prior to shaving and denuding ear skin with Nair. After prepping, the anesthetized mouse was placed on a custom designed stereotaxic restraint platform with ear bars, a nose clamp and an incisor bar to immobilize the mouse for skin imaging. A plane of deep anaesthesia was maintained using a mixture of isofluorane gas and oxygen delivered via a nosecone. Image stacks of 15 optical sections with a 400 um field of view and 3 μm z spacing were acquired every 30s for 60 – 80 minutes. The two-photon laser was tuned to a wavelength of 850 nm. Volocity software (Improvision) was used to create QuickTime formatted movies of image sequences. All movies are displayed as 2D maximum intensity projections of the time resolved image stacks. The displacement rate of cells in the four-dimensional image data sets was determined using an automatic cell tracking algorithm in Imaris software (Bitplane/Perkin Elmer). All cell tracks were individually examined to confirm that they reported the behaviour of a single cell. Only viable cells with track origins at least 10 um from an injection site were included in quantitative analysis.

Statistical analysis

We performed statistical analysis using a one-way ANOVA with a Bonferroni multiple comparison post test unless otherwise indicated. We considered $P<0.05$ to be statistically significant. Error bars represent S.E.M of samples within a group. In the case of all BAL data, the total BAL number was used to generate these error bars.

Affymetrix Array

DNA microarray analysis was performed on two independent samples of four different populations (1) WT BMDCs, (2) WT BMDCs treated overnight with LPS (1 μg/mL), (3) *Nlrp10*$^{-/-}$ BMDCs, and (4) *Nlrp10*$^{-/-}$ BMDCs treated overnight with LPS (1 μg/mL). RNA was isolated with Qiagen RNeasy MiniKit and was hybridized to Mouse Gene 1.0 ST Array (Affymetrix, Santa Clara, CA) at the Yale Keck Microarray Facility. The microarray analysis was carried out with packages in R (R Development CoreTeam, 2010). Raw microarray data in CEL file format were read in and normalized with the RMA method provided by the R oligo package. Differential gene expression was defined by two criteria: (1) an absolute fold-change ≥1.2 of knockout samples relative to WT samples and (2) a statistically significant change in expression as determined by LIMMA with a Benjamani-Hochberg false discovery rate cutoff $q < 0.05$. The microarray data discussed in this publication have been deposited in NCBI's Gene Expression Omnibus [36] and are accessible through GEO Series accession number GSE36009 (http://www.ncbi.nlm.nih.gov/geo/query/acc.cgi?acc=GSE36009).

Western blot analysis

Electrophoresis of proteins was performed with the NuPAGE system (Invitrogen) in accordance with the manufacturer's protocol. In brief, BMDCs were suspended in lysis buffer (Cell Signaling) containing a protease inhibitor cocktail (Roche). Lysates from an equal number of BMDCs were separated on a NuPAGE gel and transferred to a PVDF (poly(vinylidene difluoride)) membrane by electroblotting. To detect MMP13, rabbit polyclonal anti-MMP13 antibody (ab39012) from Abcam was used.

Supplementary Material

Refer to Web version on PubMed Central for supplementary material.

Acknowledgments

We would like to thank Ruslan Medzhitov and Matthew Albert for helpful discussion and review of this manuscript. S.C.E. was supported by T32HL007974, K08AI085038 and Yale CTSA (UL1 RR024139). O.R.C. was supported by the Damon Runyon Cancer Research Foundation (DRG 108-09), the Yale CTSA (UL1 RR024139 and 5KL2RR024138), the Yale SPORE in Skin Cancer (1 P50 CA121974) and the Dermatology Foundation. E.E. is supported by Cancer Research Institute, the American Physicians for Medicine in Israel Foundation, and the United States-Israel binational Foundation grant. A.M.H. and *in vivo* imaging supported by Yale Rheumatologic Disease Research Core Center P30AR053495. F.S.S. was supported by R01AI087630 and an Edward Mallinckrodt, Jr. Foundation scholarship. A.W. was a Howard Hughes fellow and R.A.F. is an Investigator of the Howard Hughes Medical Institute.

References

1. Takeuchi O, Akira S. Pattern recognition receptors and inflammation. Cell. 2010; 140:805–820. [PubMed: 20303872]
2. Williams A, Flavell RA, Eisenbarth SC. The role of NOD-like Receptors in shaping adaptive immunity. Curr Opin Immunol. 2010; 22:34–40. [PubMed: 20149616]
3. Medzhitov R, Janeway CA Jr. Innate immune induction of the adaptive immune response. Cold Spring Harb Symp Quant Biol. 1999; 64:429–435. [PubMed: 11232318]
4. Imamura R, et al. Anti-inflammatory activity of PYNOD and its mechanism in humans and mice. J Immunol. 2010; 184:5874–5884. [PubMed: 20393137]

5. Inohara N, Nunez G. NODs: intracellular proteins involved in inflammation and apoptosis. Nat Rev Immunol. 2003; 3:371–382. [PubMed: 12766759]
6. Wang Y, et al. PYNOD a novel Apaf-1/CED4-like protein is an inhibitor of ASC and caspase-1. Int Immunol. 2004; 16:777–786. [PubMed: 15096476]
7. Eisenbarth SC, Colegio OR, O'Connor W, Sutterwala FS, Flavell RA. Crucial role for the Nalp3 inflammasome in the immunostimulatory properties of aluminium adjuvants. Nature. 2008; 453:1122–1126. [PubMed: 18496530]
8. Li H, Willingham SB, Ting JP, Re F. Cutting edge: inflammasome activation by alum and alum's adjuvant effect are mediated by NLRP3. J Immunol. 2008; 181:17–21. [PubMed: 18566365]
9. Gris D, et al. NLRP3 plays a critical role in the development of experimental autoimmune encephalomyelitis by mediating Th1 and Th17 responses. J Immunol. 2010; 185:974–981. [PubMed: 20574004]
10. Eisenbarth SC, et al. Lipopolysaccharide-enhanced toll-like receptor 4-dependent T helper cell type 2 responses to inhaled antigen. J Exp Med. 2002; 196:1645–1651. [PubMed: 12486107]
11. Bachmann MF, Hengartner H, Zinkernagel RM. T helper cell-independent neutralizing B cell response against vesicular stomatitis virus: role of antigen patterns in B cell induction? Eur J Immunol. 1995; 25:3445–3451. [PubMed: 8566036]
12. Palm NW, Medzhitov R. Immunostimulatory activity of haptenated proteins. Proceedings of the National Academy of Sciences of the United States of America. 2009; 106:4782–4787. [PubMed: 19255434]
13. Banchereau J, Steinman RM. Dendritic cells and the control of immunity. Nature. 1998; 392:245–252. [PubMed: 9521319]
14. Ohl L, et al. CCR7 governs skin dendritic cell migration under inflammatory and steady-state conditions. Immunity. 2004; 21:279–288. [PubMed: 15308107]
15. MartIn-Fontecha A, et al. Regulation of dendritic cell migration to the draining lymph node: impact on T lymphocyte traffic and priming. J Exp Med. 2003; 198:615–621. [PubMed: 12925677]
16. Saeki H, Moore AM, Brown MJ, Hwang ST. Cutting edge: secondary lymphoid-tissue chemokine (SLC) and CC chemokine receptor 7 (CCR7) participate in the emigration pathway of mature dendritic cells from the skin to regional lymph nodes. J Immunol. 1999; 162:2472–2475. [PubMed: 10072485]
17. Itano AA, et al. Distinct dendritic cell populations sequentially present antigen to CD4 T cells and stimulate different aspects of cell-mediated immunity. Immunity. 2003; 19:47–57. [PubMed: 12871638]
18. Jakubzick C, et al. Lymph-migrating tissue-derived dendritic cells are minor constituents within steady-state lymph nodes. The Journal of experimental medicine. 2008; 205:2839–2850. [PubMed: 18981237]
19. Edelson BT, et al. Peripheral CD103+ dendritic cells form a unified subset developmentally related to CD8alpha+ conventional dendritic cells. The Journal of experimental medicine. 2010; 207:823–836. [PubMed: 20351058]
20. Ginhoux F, et al. The origin and development of nonlymphoid tissue CD103+ DCs. The Journal of experimental medicine. 2009; 206:3115–3130. [PubMed: 20008528]
21. Plantinga M, Hammad H, Lambrecht BN. Origin and functional specializations of DC subsets in the lung. Eur J Immunol. 2010; 40:2112–2118. [PubMed: 20853496]
22. Cyster JG. Chemokines sphingosine-1-phosphate and cell migration in secondary lymphoid organs. Annual review of immunology. 2005; 23:127–159.
23. Czeloth N, Bernhardt G, Hofmann F, Genth H, Forster R. Sphingosine-1-phosphate mediates migration of mature dendritic cells. J Immunol. 2005; 175:2960–2967. [PubMed: 16116182]
24. Dieu MC, et al. Selective recruitment of immature and mature dendritic cells by distinct chemokines expressed in different anatomic sites. The Journal of experimental medicine. 1998; 188:373–386. [PubMed: 9670049]
25. Gunn MD, et al. Mice lacking expression of secondary lymphoid organ chemokine have defects in lymphocyte homing and dendritic cell localization. The Journal of experimental medicine. 1999; 189:451–460. [PubMed: 9927507]

26. Sallusto F, et al. Rapid and coordinated switch in chemokine receptor expression during dendritic cell maturation. Eur J Immunol. 1998; 28:2760–2769. [PubMed: 9754563]
27. Noben-Trauth N, et al. An interleukin 4 (IL-4)-independent pathway for CD4+ T cell IL-4 production is revealed in IL-4 receptor-deficient mice. Proceedings of the National Academy of Sciences of the United States of America. 1997; 94:10838–10843. [PubMed: 9380721]
28. Zheng B, Berrie CP, Corda D, Farquhar MG. GDE1/MIR16 is a glycerophosphoinositol phosphodiesterase regulated by stimulation of G protein-coupled receptors. Proceedings of the National Academy of Sciences of the United States of America. 2003; 100:1745–1750. [PubMed: 12576545]
29. Arthur JC, et al. Cutting edge: NLRP12 controls dendritic and myeloid cell migration to affect contact hypersensitivity. J Immunol. 2010; 185:4515–4519. [PubMed: 20861349]
30. Ippagunta SK, et al. The inflammasome adaptor ASC regulates the function of adaptive immune cells by controlling Dock2-mediated Rac activation and actin polymerization. Nature immunology. 2011; 12:1010–1016. [PubMed: 21892172]
31. Sutterwala FS, et al. Critical role for NALP3/CIAS1/Cryopyrin in innate and adaptive immunity through its regulation of caspase-1. Immunity. 2006; 24:317–327. [PubMed: 16546100]
32. Cohn L, Homer RJ, Niu N, Bottomly K. T helper 1 cells and interferon gamma regulate allergic airway inflammation and mucus production. J Exp Med. 1999; 190:1309–1318. [PubMed: 10544202]
33. Laouar Y, et al. TGF-beta signaling in dendritic cells is a prerequisite for the control of autoimmune encephalomyelitis. Proc Natl Acad Sci U S A. 2008; 105:10865–10870. [PubMed: 18669656]
34. Lutz MB, et al. An advanced culture method for generating large quantities of highly pure dendritic cells from mouse bone marrow. J Immunol Methods. 1999; 223:77–92. [PubMed: 10037236]
35. Jakubzick C, Helft J, Kaplan TJ, Randolph GJ. Optimization of methods to study pulmonary dendritic cell migration reveals distinct capacities of DC subsets to acquire soluble versus particulate antigen. J Immunol Methods. 2008; 337:121–131. [PubMed: 18662693]
36. Edgar R, Domrachev M, Lash AE. Gene Expression Omnibus: NCBI gene expression and hybridization array data repository. Nucleic Acids Res. 2002; 30:207–210. [PubMed: 11752295]

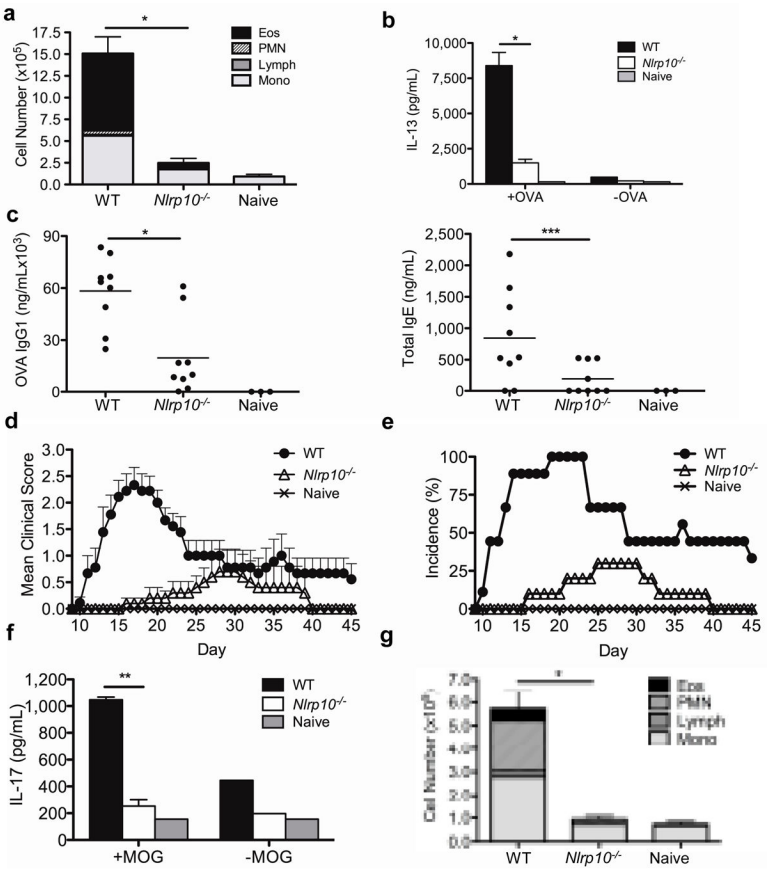

Figure 1. *Nlrp10*$^{-/-}$ mice have a global defect in adaptive immune responses

a, Bronchoalveolar lavage **b,** mediastinal lymph node culture IL-13 and **c,** serum antibodies from WT and *Nlrp10*$^{-/-}$ mice sensitized intraperitoneally with OVA/alum and challenged intranasally with OVA (n=4–5 mice/group from one of five independent experiments). **d,** Mean clinical paralysis score **e,** percent of mice with paralysis and **f,** lymph node culture IL-17 from WT and *Nlrp10*$^{-/-}$ mice following sensitization with MOG/CFA and Pertussis Toxin (n=8–10 mice from one of three independent experiments). P<0.0001 WT vs. *Nlrp10*$^{-/-}$ by one way ANOVA. **g,** Bronchoalveolar lavage from WT and *Nlrp10*$^{-/-}$ mice sensitized and challenged intranasally with OVA (n=3–5 mice/group). * *P*<0.0001; ** *P*<0.001; *** *P*<0.023. All error bars S.E.M.

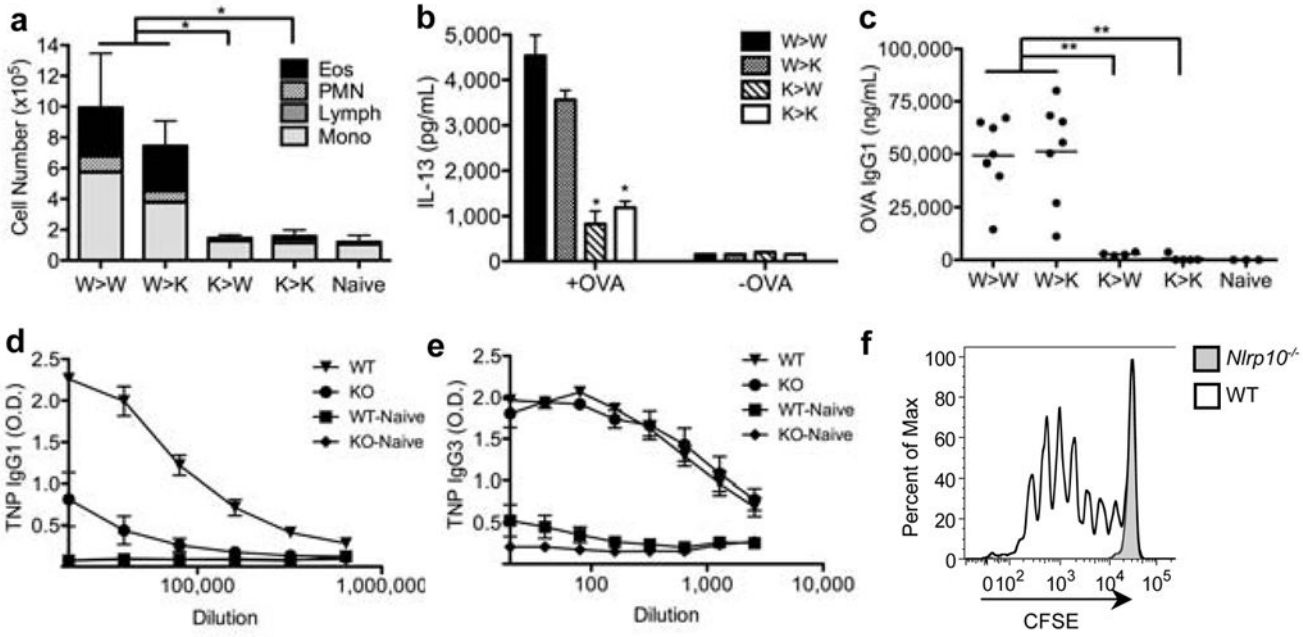

Figure 2. *Nlrp10*$^{-/-}$ mice cannot mount T cell dependent adaptive immune responses

a, Bronchoalveolar lavage **b**, mediastinal lymph node culture and **c**, serum antibody from bone marrow chimeras (Donor>Recipient, W=WT, K=*Nlrp10*$^{-/-}$) immunized and challenged as in figure 1a–c (n=4–6 mice/group from one of three independent experiments). **d**, Serum TNP-specific IgG1 in TNP-KLH immunized WT or *Nlrp10*$^{-/-}$mice. $P<0.0022$ by one way ANOVA, (KO=*Nlrp10*$^{-/-}$). **e**, TNP-specific IgG3 in TNP-Ficoll immunized mice (n=3–5 mice/group from one of two independent experiments, KO=*Nlrp10*$^{-/-}$). **f**, CFSE dilution of labelled WT OVA-specific OTII T cells in the draining lymph node of WT or *Nlrp10*$^{-/-}$ hosts three days following OVA/LPS immunization. One of three mice/group is shown. *$P<0.033$, **$P<0.0001$. All error bars S.E.M.

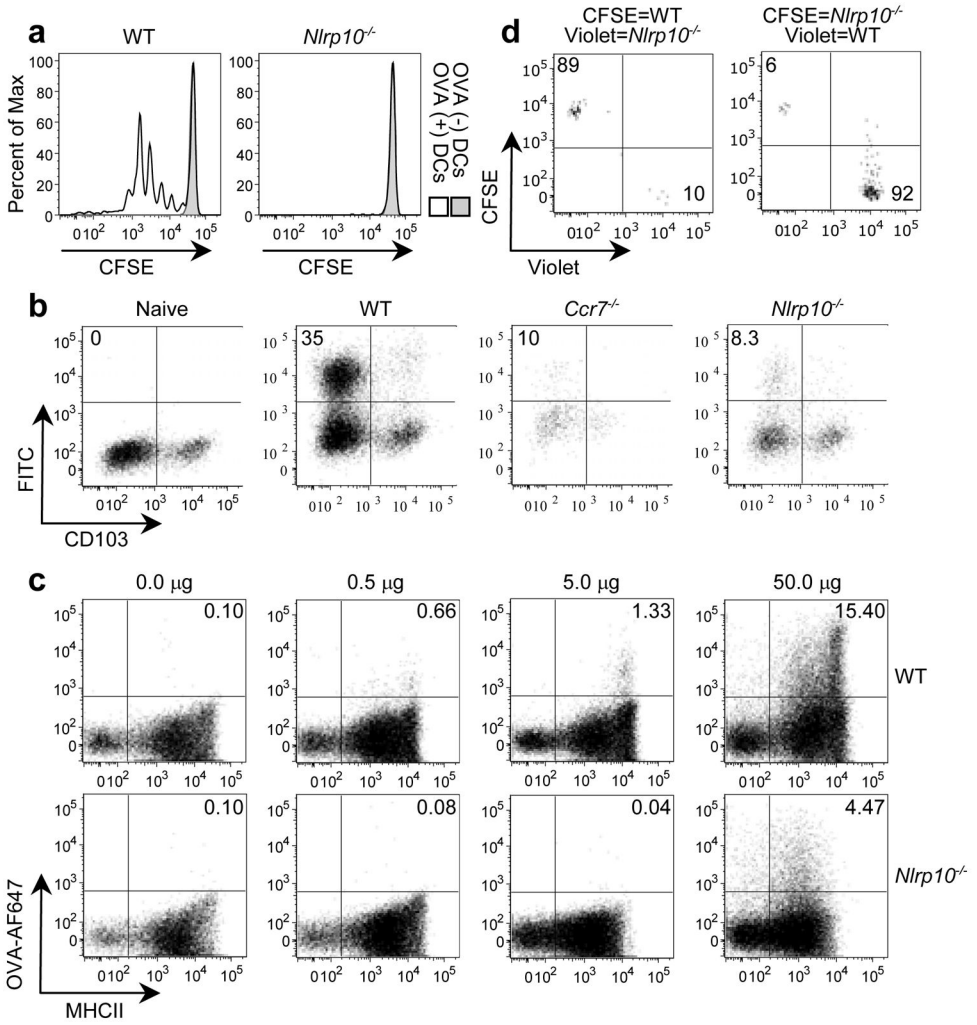

Figure 3. *Nlrp10*$^{-/-}$ dendritic cells do not take antigen to the draining lymph node

a, Dilution of lymph node CFSE^{+} OTII T cells adoptively transferred into WT hosts three days after injection with WT or *Nlrp10*$^{-/-}$ OVA peptide pulsed (solid line) or unpulsed (shaded histogram) BMDCs. One of three mice/group is shown. **b**, FITC^{+} CDllc^{+}MHCII^{hi} DCs in the draining LN of WT, *Ccr7*$^{-/-}$ or *Nlrp10*$^{-/-}$ mice painted with 1% FITC. One representative experiment of four. **c**, CD11b^{+}CD11c^{+} DCs in the LN of WT or *Nlrp10*$^{-/-}$mice injected with indicated doses of OVA-AF647 with LPS. One of three mice/group is shown. **d,** WT and *Nlrp10*$^{-/-}$ BMDCs were labelled with CFSE or CellTrace Violet and co-injected into CD45.1 mice with LPS. Inguinal lymph nodes were analysed for CD45.2^{+}CD11c^{+}MHCII^{+} BMDCs. One of two mice/group from one experiment of seven.

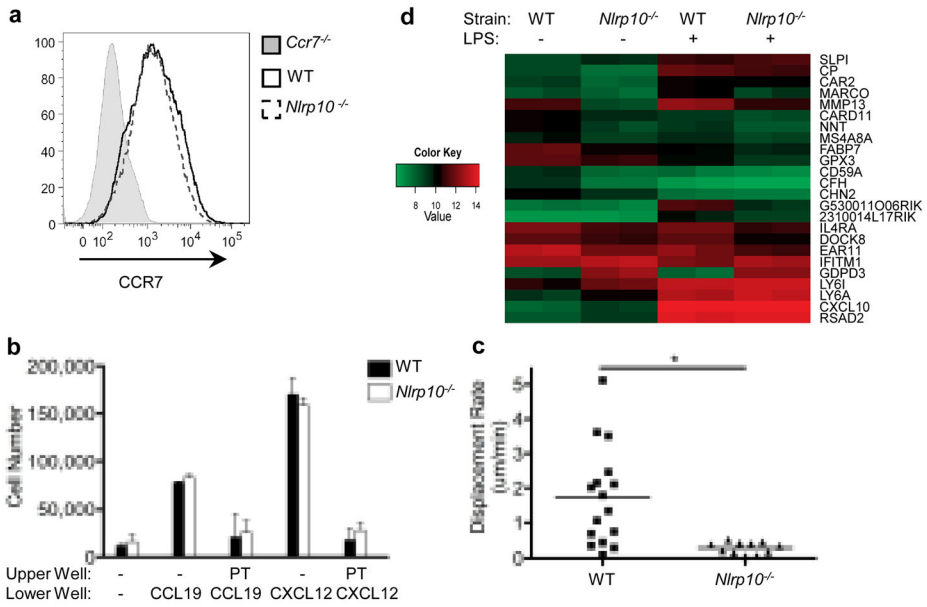

Figure 4. *Nlrp10*$^{-/-}$ dendritic cells cannot emigrate from inflamed tissue but remain responsive to chemokines

a, CCR7 surface expression on WT, *Ccr7*$^{-/-}$ or *Nlrp10*$^{-/-}$BMDCs stimulated with LPS. One representative experiment of two. **b,** Number of WT or *Nlrp10*$^{-/-}$ LPS-treated BMDCs that migrated in a transwell to CCL19 or CXCL12. Control BMDCs were treated with pertussis toxin (PT) before use. Representative of three experiments. All error bars S.E.M. **c,** Cell track displacement rate of BMDCs labelled with CMTMR (WT) or CFSE (*Nlrp10*$^{-/-}$) co-injected into the ears of WT hosts and imaged 4 hours later by intravital two-photon laser scanning microscopy; **P*<0.0012. **d,** Heat map of log2 transformed gene expression values in *Nlrp10*$^{-/-}$ and WT BMDCs treated with and without LPS.